

ARTICLE

Open Access



A free elution immunoassay for chloramphenicol in chicken and egg after magnetic ZIF-8 adsorption separation

Liang Zhang^{1†}, Sihan Wang^{1,2†}, Jincheng Xiong¹, Yuliang Xv¹, Jie Xie³, Zhanhui Wang^{1,2}, Congming Wu¹, Haiyang Jiang^{1,2*}  and Jianzhong Shen^{1,2*}

Abstract

The excellent adsorption and rapid separation capabilities of magnetic MOFs make them desirable pretreatment materials for solid substrates. In this study, magnetic ZIF-8 (mZIF-8) was synthesized in situ by a one-step method in the aqueous solution of magnetic beads. Isothermal adsorption verified that the maximum adsorption capacity of (011) crystal-exposed rhombic dodecahedral ZIF-8 for chloramphenicol was up to 128.31 mg/g (mZIF-8 = 67.18 mg/g). Kinetic adsorption revealed that the type of ZIF-8/mZIF-8 adsorption on chloramphenicol belongs to the pseudo-secondary adsorption kinetics of chemical monomolecular layers. Characterization by FTIR, XPS, and XRD revealed that mZIF-8 interacts with chloramphenicol mainly by π - π electron stacking, electrostatic attraction, and hydrogen bonding interaction. ELISA confirmed that chloramphenicol remained antigenically active after adsorption by mZIF-8. The adsorption and separation of chloramphenicol residues in chicken and egg were completed by mZIF-8 within 20 min. mZIF-8 can be used directly for elution-free ELISA after the adsorption of chloramphenicol. The limits of detection (IC_{10}) of the mZIF-8 + ELISA in chicken and eggs were 1.18 ng/mL and 0.64 ng/mL, respectively. mZIF-8 is expected to be used as a magnetic solid-phase extraction material for the rapid pretreatment of antibiotic residues in other complex solid matrices.

Keywords Magnetic metal-organic frameworks, Pretreatment, Elution-free, Chloramphenicol, Enzyme-linked immunosorbent assay

[†]Liang Zhang and Sihan Wang contributed equally to this work.

*Correspondence:

Haiyang Jiang

haiyang@cau.edu.cn

Jianzhong Shen

sjz@cau.edu.cn

¹ Department of Veterinary Pharmacology and Toxicology, National Key Laboratory of Veterinary Public Health Security, Beijing Key Laboratory of Detection Technology for Animal-Derived Food Safety, Beijing Laboratory for Food Quality and Safety, College of Veterinary Medicine, China Agricultural University, Beijing 100193, China

² Technology Innovation Center for Food Safety Surveillance and Detection, Sanya Institute of China Agricultural University, Hainan 572025, China

³ Technology Innovation Center of Mass Spectrometry for State Market Regulation, Center for Advanced Measurement Science, National Institute of Metrology, Beijing 100029, China

Introduction

Chloramphenicol (CAP) as a broad-spectrum antibiotic has an inhibitory effect on both aerobic Gram-positive and some Gram-negative bacteria [1]. The use of CAP in animals results in its rapid distribution to organs and edible tissues of the organism. CAP inhibits the hematopoietic function of human bone marrow and triggers aplastic anemia disorder [2]. CAP residues in animals can accumulate through the food chain and cause poisoning in humans. CAP residues in animals can accumulate through the food chain and cause poisoning in humans. Therefore, CAP is banned for use in edible animal farming in China, the United States, and the European Union, among others [3, 4]. Chloramphenicol has an excellent



antimicrobial effect and low cost of use, therefore illegal use of CAP in poultry farming often occurs. The monitoring of CAP residues in poultry and egg products is important to ensure food safety.

Sample pretreatment consumes 60% of the total assay time [5], and the effect of pretreatment directly affects the accuracy and sensitivity of the assay. Currently, the extraction of residual compounds from edible tissues such as chicken and egg still relies on liquid–liquid extraction and solid-phase extraction. Solid phase extraction is more suitable for the extraction of compounds from solid matrices such as organs and tissues because no phase separation is required and less organic solvent is consumed [6]. Superparamagnetic nanoparticles (SMNPs) can be rapidly attracted by magnetic fields and do not retain their magnetism when the magnetic field is removed. Therefore, after the target adheres to the surface of SMNPs, the rapid separation of the target in the matrix under the action of the external magnetic field can be achieved without causing agglomeration [7]. Thus, magnetic solid-phase extraction can simplify the solid sample pretreatment steps and significantly reduce the pretreatment time. In particular, SMNPs modified adsorbent materials (physical, biological) can achieve selective adsorption on the target.

Metal–organic frameworks (MOFs) are porous polymers made of metal centers ligated with organic ligands, which have huge specific surface areas and ultra-high porosity [8]. ZIF-8 (zeolitic imidazolate framework) has the high adsorption properties typical of MOFs materials and also has favorable stability to organic solvents and aqueous solutions [9]. The crystal structure of MOFs is regulated by controlling the synthesis of organic ligands in MOFs to obtain special adsorption properties of MOFs. Controlling the crystal size and reducing the pore volume of ZIF-8 helps it to adsorb *n*-butanol [10]. By regulating the liquid-phase crystallization process of ZIF-8, RD-ZIF-8 with a rhombic dodecahedron crystal structure was obtained. The resulting RD-ZIF-8 has a high affinity for proteins (ADAM17cyto) [11]. Therefore, controlling the crystal conformation of ZIF-8 to obtain its target-specific adsorption properties is a desirable modification strategy.

In this study, the negatively charged magnetic nanoparticles (MNPs) were first prepared by the co-precipitation method. Magnetic ZIF-8 (mZIF-8) with external MNPs on the surface of ZIF-8 crystals was obtained by one-step in situ self-assembly in the aqueous phase by controlling the organic ligand equivalents of ZIF-8. The adsorption properties of mZIF-8 on chloramphenicol in different matrices were obtained by adsorption thermodynamic and kinetic tests. The possible adsorption mechanism of mZIF-8 on CAP was further investigated using infrared

and X-ray electron spectroscopy techniques. The rapid enrichment and separation of CAP in chicken and egg were accomplished by optimizing the ELISA pre-treatment system using mZIF-8. Eventually, an ELISA residue detection method for CAP without elution based on mZIF-8 as pre-treatment material was established (Sch. 1).

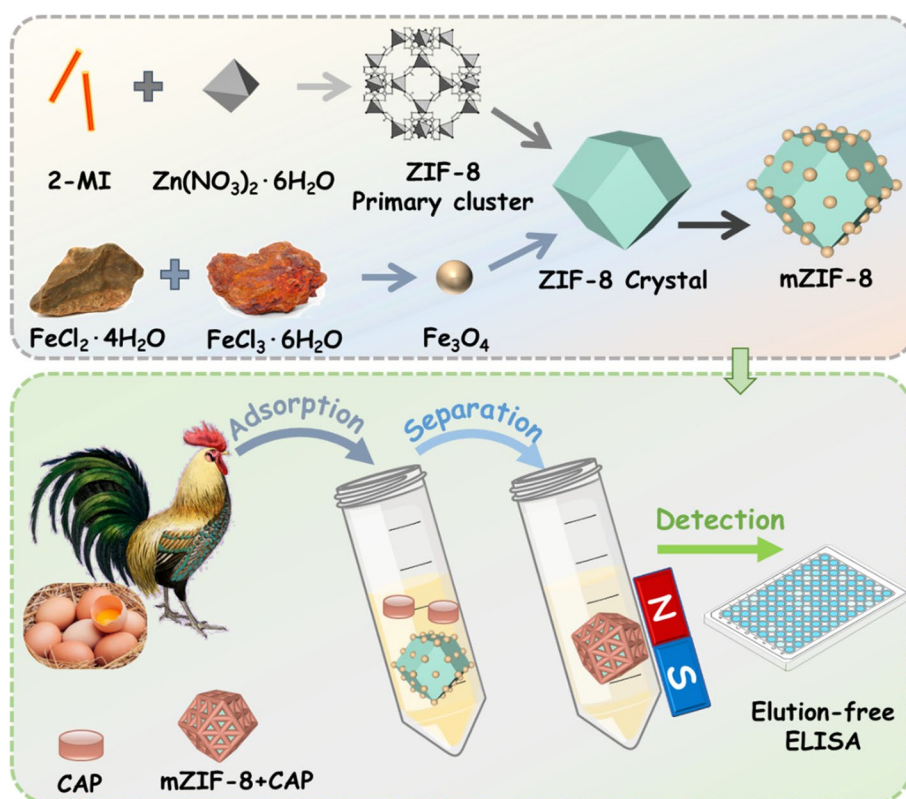
Results and discussion

Characterization of mZIF-8

The evolution of the mZIF-8 crystal morphology is shown schematically in Fig. 1a. Initially, the cubes formed in the (001) crystal orientation, when the ZIF-8 crystal particles are the smallest, with a particle size of about 50–70 nm (Fig. 1b). As the crystallization process continues, truncated rhombic dodecahedra ZIF-8 (TRD-ZIF-8) with (001) and (011) crystal orientations appear. As shown in Fig. 1c, the particle size of TRD-ZIF-8 is about 500 nm. According to Wulff's rule, the slowest-growing crystal facets is the most stable crystal structure [12]. ZIF-8 eventually forms a rhombic dodecahedron (RD-ZIF-8) with stable (011) crystal facets (Fig. 1d). Since this process is carried out in an aqueous solution of magnetic nanoparticles (MNPs). While synthesizing ZIF-8 in situ, the MNPs self-assemble on the ZIF-8 crystal surface to form magnetic ZIF-8 particles (mZIF-8) (Fig. 1e). The elemental distribution scan of mZIF-8 particles revealed that they are mainly composed of five elements, Zn, O, C, N, and Fe (Fig. 1f).

Speculation on the mechanism of mZIF-8 adsorbing CAP

The size of mZIF-8 particles was tested and found to be normally distributed, with the average particle size mainly concentrated at 577 nm (Fig. 2a). Zeta potential tests yielded positive charges for both ZIF-8 and mZIF-8 particles (Fig. 2b). The magnetic characterization of mZIF-8 showed it is well superparamagnetic with a magnetic field strength of 0.156 emu/g (Fig. 2c). XRD, XPS, and FTIR characterization of mZIF-8 after adsorption of CAP were performed to investigate their possible adsorption mechanism. Figure 2d shows that mZIF-8 has the same crystal diffraction angle as ZIF-8 (2θ angle at 7.28° represents $\langle 011 \rangle$ crystal facets). mZIF-8 also did not show a new crystal orientation angle after the adsorption of CAP, indicating that the crystal morphology of mZIF-8 did not change after the adsorption of CAP. The XPS characterization revealed that the elemental composition of mZIF-8 added Fe element (Fe2p) to the original one of ZIF-8 (Zn, O, C, and N elements). After the adsorption of CAP by mZIF-8, a peak of elemental chlorine (Cl2p) appeared at the binding energy at 200.77 eV, indicating that chemisorption of chloramphenicol with mZIF-8 occurred (Fig. 2e). The blue shift of the main peak of the imidazole ring in mZIF-8 from 1423 cm^{-1} to 1421 cm^{-1} , and the red shift of the C=C vibration in the benzene ring of CAP from



Scheme 1 The Schematic diagram of elution-free ELISA based on mZIF-8 extraction of CAP

1579 cm^{-1} to 1592 cm^{-1} after the adsorption of mZIF-8 to CAP indicate the π - π electron interaction between the imidazole ring of mZIF-8 and the benzene ring of CAP molecule (Fig. 2f). After the zeta potential test, mZIF-8 was positively charged and CAP was negatively charged. mZIF-8 adsorbed CAP with an overall positive charge, thus indicating the existence of electrostatic interactions between mZIF-8 and CAP (Fig. 2b). Molecular docking simulations (Fig. 2g) reveal a weak interaction of the H in mZIF-8 with the O in the CAP molecule by hydrogen bonding (The hydrogen bond angle is 147.686° and the bond length is 2.091 nm). Further characterization of the elemental distribution of mZIF-8 after adsorption of CAP using SEM-EDS verified that the surface of mZIF-8 material after adsorption of CAP has a large distribution of chlorine elements (Fig. 2h and i). In summary, the possible adsorption mechanisms of mZIF-8 on CAP are mainly composed of π - π electron stacking, electrostatic attraction, and hydrogen bonding interactions.

Adsorption performance of mZIF-8 on CAP

The maximum adsorption capacities of ZIF-8 and mZIF-8 on CAP were tested by isothermal adsorption tests. The maximum adsorption capacity of ZIF-8 on CAP was 128.31 mg/g (Tab. S1). The maximum adsorption capacities of mZIF-8 for CAP in water, chicken

meat, and eggs were 67.18, 40.67, and 48.35 mg/g, respectively. The adsorption model of ZIF-8 on CAP is more consistent with the Langmuir model (Fig. S2a). The type of adsorption of mZIF-8 to CAP in different matrices is also closer to the Langmuir model (Fig. 3a-c). Therefore, the adsorption results of Langmuir indicate that the adsorption of ZIF-8 and mZIF-8 on CAP belongs to monomolecular layer adsorption. The adsorption rate of the MOFs to CAP was further tested by adsorption kinetic tests. The adsorption profile of ZIF-8 on CAP was more consistent with the pseudo second-order adsorption kinetics (Fig. S2b). The adsorption curves of mZIF-8 on CAP in three matrices (water, chicken, and egg) continued to be more consistent with pseudo second-order adsorption kinetics (Fig. 3d-f). The equilibrium time for the adsorption of ZIF-8 on CAP in water was about 184 min; The equilibration time of mZIF-8 for CAP adsorption in different matrices was in the range of 168–240 min. The results of pseudo second-order adsorption kinetics indicate that the adsorption of ZIF-8 and mZIF-8 on CAP is chemisorption (The adsorption kinetic results are detailed in Tab. S2).

Pretreatment method optimization

Optimizing the dosage of the adsorbent and the adsorption time on the target directly affects the

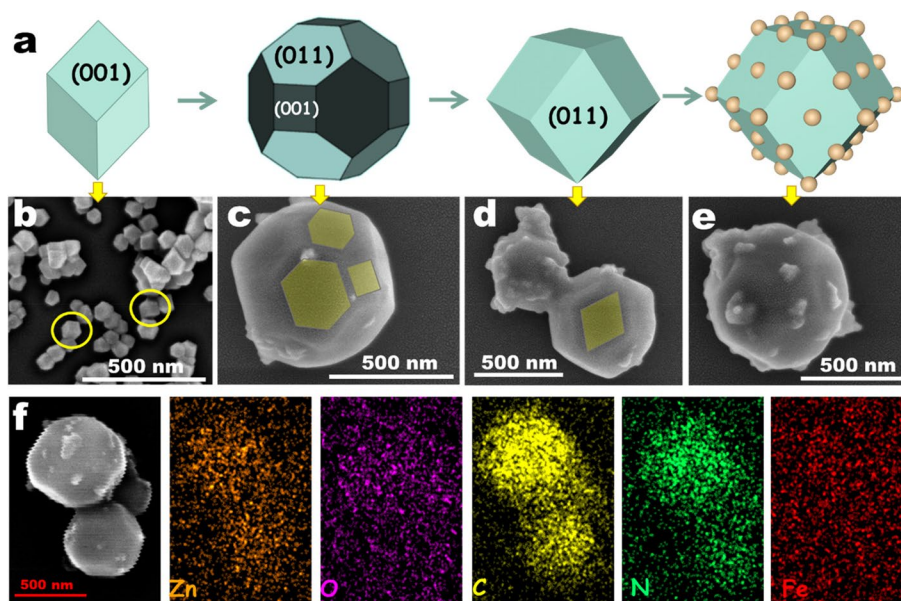


Fig. 1 The Microscopic morphology of mZIF-8. **a** Schematic diagram of mZIF-8 crystal growth with (011) crystal surface facets; **b** SEM of rhombic hexahedral ZIF-8 crystals with (001) crystal faces; **c** SEM of truncated rhombic dodecahedra ZIF-8 crystals with (001) and (011) crystal faces; **d** SEM of rhombic dodecahedra ZIF-8 crystals with (011) crystal faces; **e** Magnetic rhombic dodecahedral ZIF-8 crystals; **f** SEM-EDS characterization of mZIF-8

efficiency of the pretreatment. In addition, evaluating the conditions of use of the adsorbent based on possible interferences during sample testing is also critical to the performance of the pretreatment material. Optimization of the pretreatment conditions resulted in a dosage of mZIF-8 of 2.0 mg/mL and an adsorption time of 20 min (Fig. 4a and b). The optimal pH of the adsorption system is 7.0 (Fig. 4c), and the NaCl salt solution with a concentration of 0–0.5 M has a weak effect on the adsorption effect (Fig. 4d). The optimal amount of mZIF-8 adsorbed CAP in chicken and egg was 2.0 mg/mL (Fig. 4e), and the adsorption time was 20, and 30 min, respectively (Fig. 4f).

Elution-free ELISA methodological validation

The IC_{50} of the ELISA with PBS solution as the quality control group was 0.78 ng/mL, and the detection range (IC_{20} – IC_{80}) was 0.22–2.79 ng/mL (Fig. 5a). The IC_{50} of the elution-free ELISA method after adsorption of CAP in water by mZIF-8 was 1.55 ng/mL, and the detection range (IC_{20} – IC_{80}) was 0.44–5.46 ng/mL (Fig. 5b). The IC_{50} in chicken and egg were 2.88 and 2.61 ng/mL; the detection ranges were 1.31–6.33 ng/mL and 1.20–5.66 ng/mL, respectively. In addition, comparing the conventional ELISA method that requires an elution procedure with the elution-free ELISA, the IC_{50} of the elution-ELISA is 1.13 ng/mL

(Fig. 5c) (More ELISA results are shown in Tab. S3). The accuracy of the two ELISA methods was assessed by the recovery rate. The recoveries of the elution-free ELISA for the detection of CAP in chicken and eggs were 80.43%–92.55% and 82.46%–94.95%, respectively (Fig. 5d). The recoveries of the elution-ELISA for the detection of CAP in chicken and eggs were 84.87%–97.56% and 88.09%–98.42%, respectively (Fig. 5e). The RSD of the test results for the recoveries of all three concentrations (1.0, 5.0, and 10 ng/mL) were within 10% ($n=3$). The above results indicate that mZIF-8 as a pretreatment material can meet the requirements of ELISA (Elution-free or Elution) for CAP in chicken and eggs.

Comparing the results of this study with those of recent CAP assays (Table 1), it can be found that mZIF-8 has a high adsorption capacity and rapid adsorption efficiency for CAP. The elution-free ELISA for mZIF-8 is less time-consuming and more sensitive than other immunological rapid assays. More importantly, mZIF-8 has a more efficient pre-treatment capability for solid edible animal tissues. The specificity test of mZIF-8 elution-free ELISA for CAP is shown in Fig. S3.

Actual sample detection

Twelve real samples of chicken and eggs were pretreated using mZIF-8 and subjected to an elution-free ELISA based on the principle of double-blind experiments.

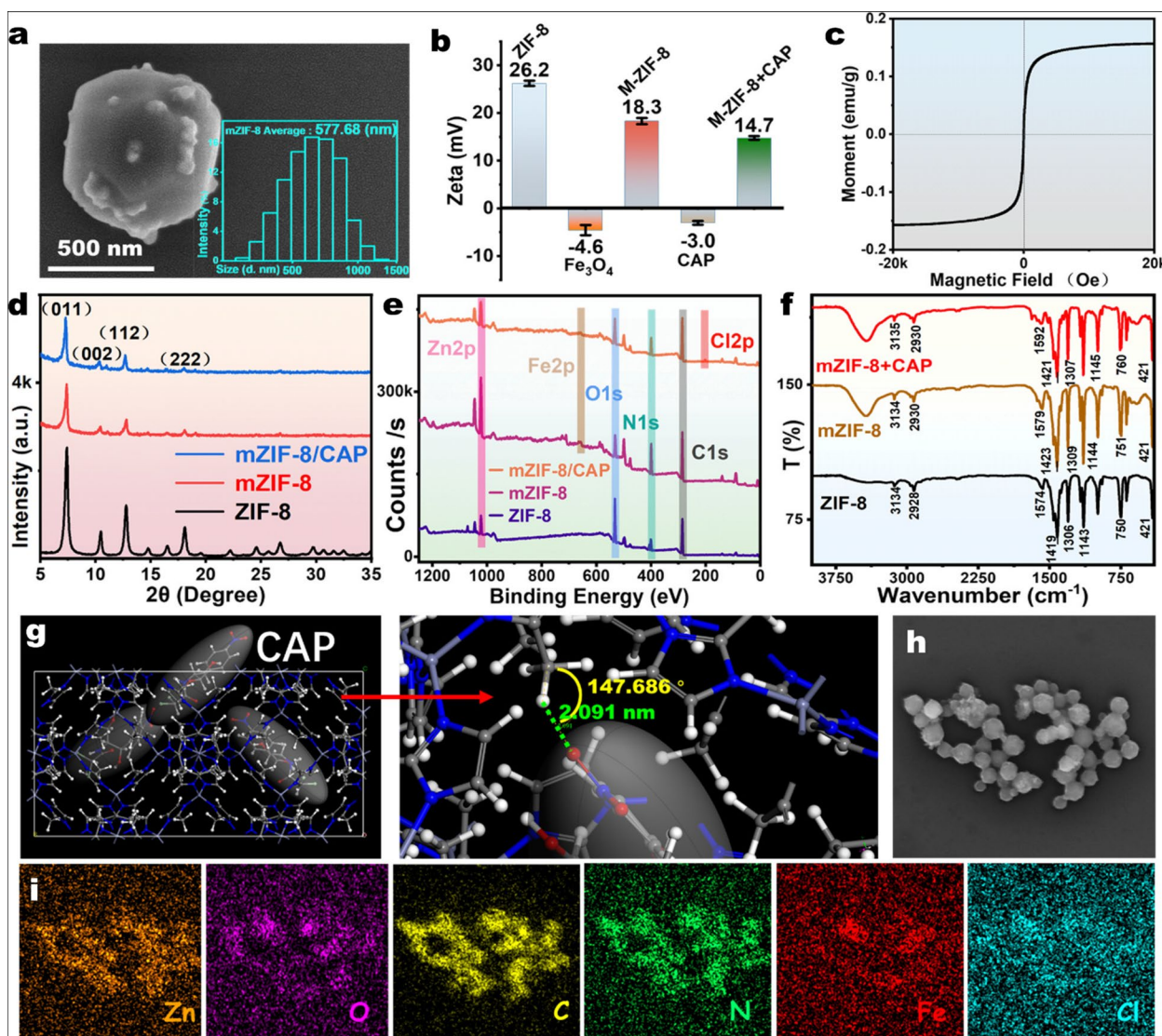


Fig. 2 Characterization of mZIF-8 and its adsorption to CAP. **a** SEM and DLS measurement of mZIF-8; **b** Zeta potential measurement with mZIF-8 and CAP; **c** Magnetization curve of mZIF-8; **d** XRD pattern of mZIF-8 adsorbed CAP; **e** XPS pattern of mZIF-8 adsorbed CAP; **f** FTIR spectrum of mZIF-8 adsorbed CAP; **g** Simulation of hydrogen bonding between mZIF-8 crystals and CAP molecules; **h** SEM image of mZIF-8 adsorbed CAP; **i** EDS pattern of mZIF-8 adsorbed CAP

The accuracy of all samples tested ranged from 91.0% to 114.1%, and all results were without false negatives and false positives (Tab. S4). The above results indicate that mZIF-8 is suitable for the pretreatment of chloramphenicol in chicken and eggs, and that chloramphenicol in the matrix can be directly determined by ELISA without elution after adsorption and magnetic separation. LC-MS/MS validation was performed on samples collected after elution using the organic mobile phase (Fig. S3). Local commercially available chicken and egg samples from Sanya City, Hainan Province tested negative for CAP (Tab. S5).

Conclusion

This study reveals that rhombic dodecahedral ZIF-8 with (011) crystalline surface facets has selective adsorption to chloramphenicol. Magnetic ZIF-8 was successfully prepared in the aqueous phase and used for the adsorption and rapid separation of chloramphenicol from chicken meat and eggs. FTIR, XRD, XPS, and Zeta potential characterization indicated that mZIF-8 adsorbed chloramphenicol mainly through π - π electron stacking, hydrogen bonding, and electrostatic interaction. Owing to the high adsorption characteristics of ZIF-8 (large specific surface area) and the magnetic separation ability of the beads,

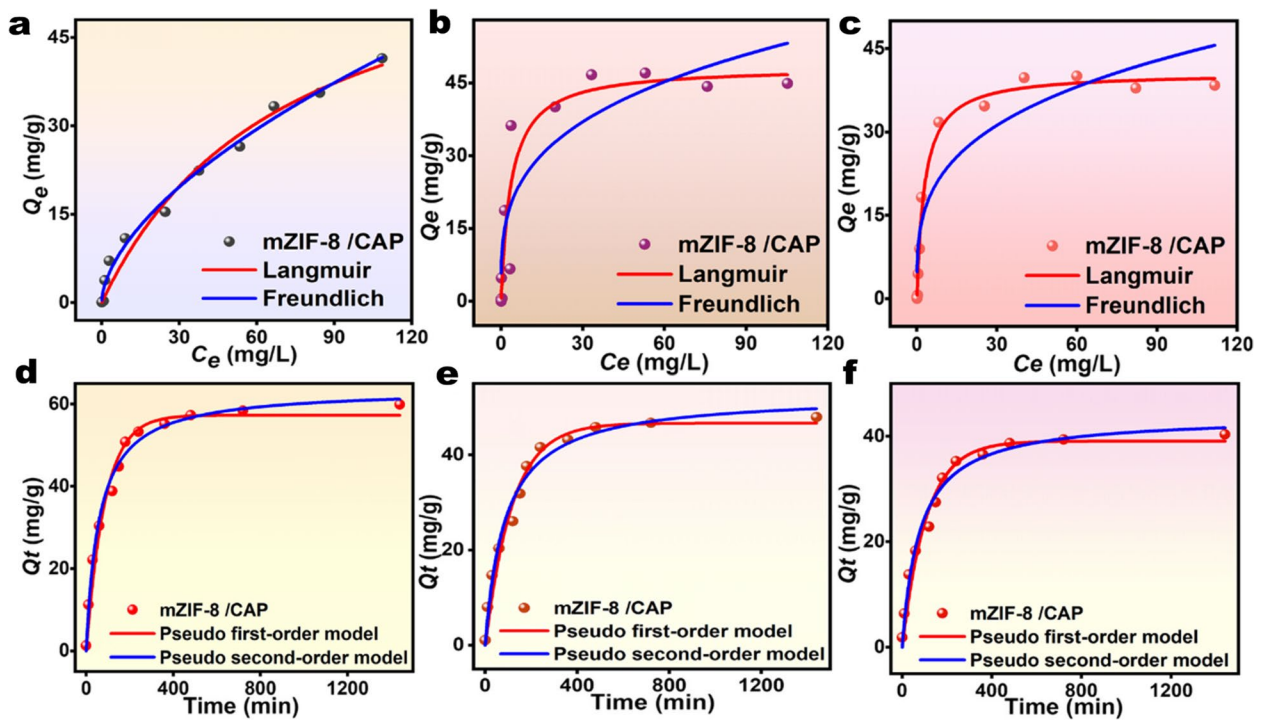


Fig. 3 mZIF-8 adsorption performance test. **a** Isothermal adsorption curve of mZIF-8 on CAP in water; **b** Isothermal adsorption curves of mZIF-8 on CAP in egg; **c** Isothermal adsorption curves of mZIF-8 on CAP in chicken; **d** Kinetic adsorption curves of mZIF-8 on CAP in water; **e** Kinetic adsorption curves of mZIF-8 on CAP in egg; **f** Kinetic adsorption curves of mZIF-8 on CAP in chicken

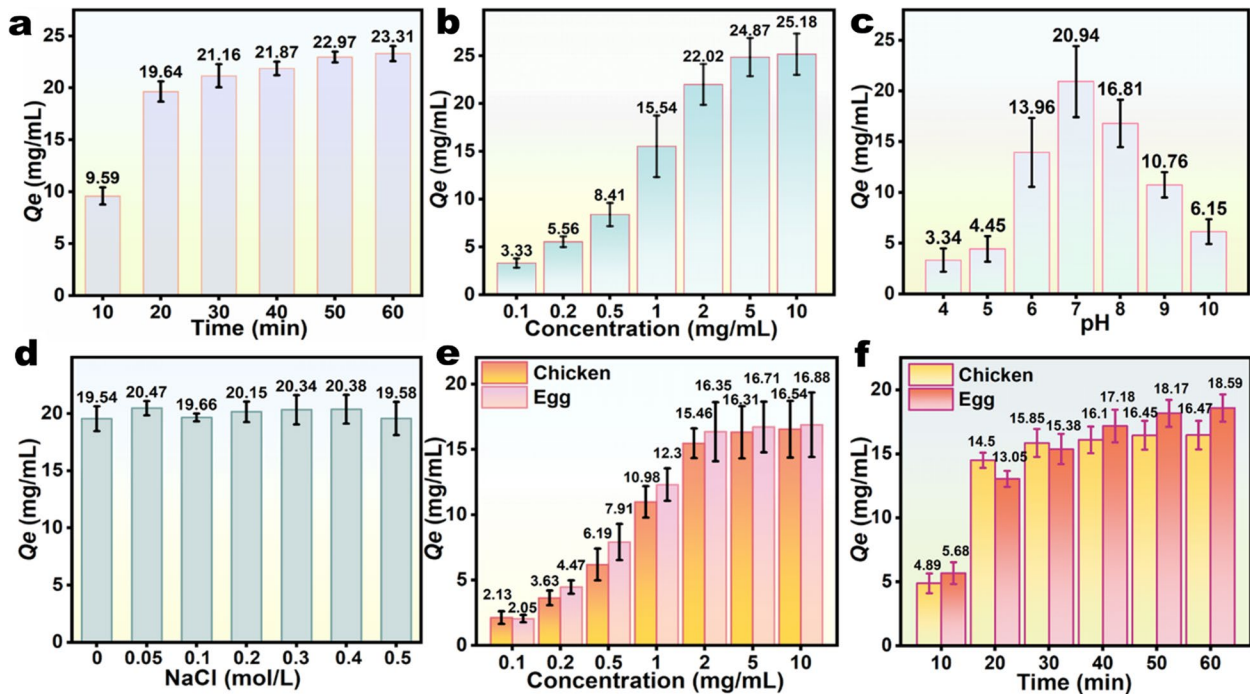


Fig. 4 Optimization of sample pretreatment conditions based on mZIF-8. **a** Adsorption time optimization; **b** Optimization of adsorbent (mZIF-8) dosage; **c** pH optimization of the adsorption system; **d** Effect of salt ion strength on adsorption; **e** Optimization of mZIF-8 dosage in chicken and eggs; **f** Optimization of mZIF-8 adsorption time in chicken and eggs

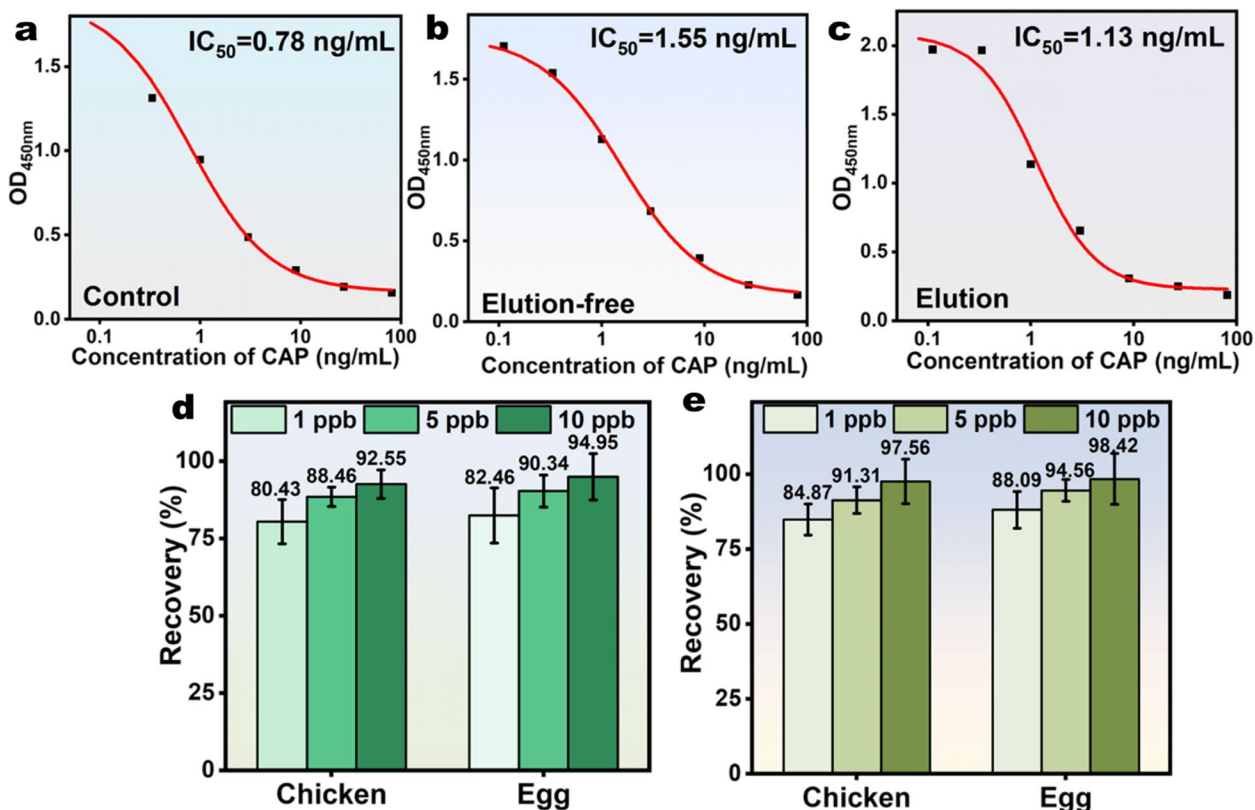


Fig. 5 The ELISA standard curve and recovery of mZIF-8. **a** ELISA standard curve in standard solution (PBS); **b** Elution-free ELISA standard curve; **c** ELISA standard curve requiring elution procedure; **d** Recovery of elution-free ELISA; **e** Recovery of ELISA with elution procedure

Table 1 Comparison of mZIF-8 with other CAP assays

Pretreatment materials/ Probes	Samples	Method	Adsorption Capacity (mg/g)	Pretreatment	LOD	Reference
MIP/Zr-LMOF	Milk & Honey	LC-MS/MS	/	TCA + EA + MeOH liquid-liquid extraction > 30 min	0.013 $\mu\text{g/L}$	[13]
AuNPs	Water	Lateral Flow Immunochromatographic Strips	/	/ (No pre-treatment required for water samples)	63.4 ng/mL	[14]
Si@MIPs-CAP	Water	UV/Vis	32.26	/	/	[15] ^a
Structure-switching signaling aptamer	Milk	FRET	/	TCA + TM liquid-liquid extraction 1.5 h	0.71 ng/mL	[16] ^a
PCN-222	Water	UV/Vis	370	/	/	[17]
microporous nanofibrous membranes	Salmon	nanofibrous ELISA	/	\approx 50 min	0.3 ng/mL	[18]
paper-based antibiotic sensor	Milk/Fish	ELISA	/	60 min	0.05 ng/mL	[19]
molecularly imprinted graphene	Meat	CRET-ELISA ^b	/	38 min	0.1 ng/mL	[20]
mZIF-8 (011) Crystals	Chicken/Egg	Free-elution ELISA	67.18	20 min Reagent elution-free	1.18 ng/mL/ 0.64 ng/mL	In this study

/: Not mentioned in the literature

^a: Adsorption studies, no actual samples tested

^b: Chemiluminescence Resonance Energy Transfer platform

mZIF-8 accomplished sufficient adsorption of chloramphenicol from animal-derived foods (chicken & egg) within 20 min. ELISA confirmed that chloramphenicol remained antigenically immunoreactive after adsorption by mZIF-8. The elution-free ELISA method with mZIF-8 as pretreatment material simplifies the pretreatment steps and shortens the pretreatment time for solid sample matrices, while achieving similar sensitivity to conventional ELISA methods for chloramphenicol detection. Magnetic MOFs hold promise as solid-phase extraction materials for the pretreatment of other antibiotic residues in animal-derived foods.

Materials and methods

Synthesis and characterization of MOFs

Magnetic beads were prepared by the co-precipitation method [21]. Magnetic ZIF-8 particles (mZIF-8) were obtained by one-step self-assembly in an aqueous magnetic bead solution. Materials and the detailed preparation steps are described in the [supplementary materials](#). Monoclonal antibodies and encapsulated antigens for CAP were made homemade for this experiment [22].

Characterization of mZIF-8 adsorbed CAP

Microscopic morphology and elemental distribution of mZIF-8 crystals were observed by field emission Scanning Electron Microscopy (SEM) tandem Energy Dispersive Spectrometer (EDS); The particle size distribution and zeta potential of mZIF-8 were measured using dynamic light scattering (DLS); The magnetic properties of mZIF-8 were determined using Vibrating Sample Magnetometer (VSM); X-ray Diffraction (XRD), X-ray Photoelectron Spectroscopy (XPS) and Fourier Transform Infrared Reflection (FTIR) was used to observe the changes of crystal orientation, elemental valence and chemical groups of mZIF-8 after adsorption of CAP, respectively.

Adsorption performance of mZIF-8 for CAP

Isothermal adsorption test at 298 K — Activation of mZIF-8 for 8 h at 80 °C under vacuum. 25 mg of mZIF-8 was dispersed in an aqueous CAP solution at concentrations of 0.1–200 mg/L. Vortex shaking for 48 h saturates mZIF-8 on CAP. After the magnetic separation of the supernatant from the completed adsorption, the remaining CAP concentration was tested using UV/Vis (Fig. S1). The isothermal adsorption curves were fitted to the adsorption data using *Langmuir* (Eq. 1) [23] and *Freundlich* (Eq. 2) [24] adsorption models, respectively. The equilibrium adsorption capacity is calculated with reference to Formula 1 (Eq. 3).

$$\text{Langmuir model : } Q_e = 1/(k_L \cdot Q_m) \cdot 1/C_e + 1/Q_m \quad (1)$$

$$\text{Freundlich model : } \ln Q_e = 1/n \ln C_e + \ln K_F \quad (2)$$

$$Q_e = (C_0 - C_e)/mV \quad (3)$$

where C_0 denotes the initial concentration of CAP solution; C_e denotes the rest concentration of CAP after adsorption equilibrium; V denotes the total volume of the adsorption system (CAP solution); m denotes the mass of adsorbent (mZIF-8); Q_m is the saturation adsorption capacity (mg/g); K_L is the Langmuir constant (L/mg); K_F is the Freundlich adsorption constant (mg/g); n is a constant.

Adsorption kinetics tests were used to evaluate the adsorption rate of mZIF-8 on CAP. The dosage of mZIF-8 was determined to be 1.0 g/L based on the data of isothermal adsorption. The concentration of CAP in the adsorption system was set to 2.0 mg/L. mZIF-8 was put into the CAP solution and fully adsorbed. The remaining CAP concentration in the system was measured at 0, 10, 30, 60, 90, 120, 150, 180, 240, 360, 480, 720, and 1440 min after adsorption, respectively. The adsorption data were fitted analytically using a pseudo-first-order adsorption kinetic model (Eq. 4) and a pseudo-second-order adsorption kinetic model (Eq. 5) [25].

$$\text{Pseudo first - order : } \ln(Q_e - Q_t) = \ln Q_e - k_1 t \quad (4)$$

$$\text{Pseudo second - order : } t/Q_t = 1/(K_2 Q_e^2) + t/Q_e \quad (5)$$

where Q_t (mg/g) is the capacity of mZIF-8 for CAP adsorption at the t (min) moment; Q_e (mg/g) denotes the adsorption capacity at which adsorption reaches equilibrium; K_1 is the pseudo first-order adsorption kinetic equilibrium constant (1/min); K_2 is the pseudo second-order adsorption kinetic equilibrium constant (g/mg·min).

Pretreatment method

A standard solution of CAP with a concentration of 30 mg/L was prepared as the working solution. The dosages of 0.1, 0.2, 0.5, 1.0, 2.0, 5.0, and 10.0 mg/mL of mZIF-8 were put into the CAP solution. After 20 min of adsorption by oscillation, the supernatant was taken by magnetic separation and the remaining CAP concentration in the supernatant was tested to calculate the optimal amount of adsorbent for mZIF-8. The optimized dosage of mZIF-8 was put into CAP solution for 10, 20, 30, 40, 50, and 60 min of oscillatory adsorption. The optimal adsorption time was screened based on the adsorption capacity. The pH of the system was adjusted to 4, 5, 6, 7, 8, 9, and 10. The adsorption capacity was determined to determine the optimum pH system. NaCl(s) was added to the adsorption system so that its concentration was 0,

0.05, 0.1, 0.2, 0.3, 0.4, 0.5 M. The effect of salt ions in the solution on the adsorption process was evaluated.

Matrix effect investigation — After weighing 2.0 g of homogenized chicken meat (egg) and adding 2.0 mL of water, the CAP solution was added after vortexing for 5 min to make the working solution concentration of 30 mg/L. The optimal dosage and adsorption time of mZIF-8 in the chicken meat (egg) matrix were optimized according to the above-optimized conditions.

Negative control samples without CAP were provided by the Veterinary Drug Safety Inspection & Testing Center of the Ministry of Agriculture (Beijing, China).

Establishment of elution-free MOF-ELISA method

The working concentration of the encapsulant and monoclonal antibody was determined by the checkerboard method, with the encapsulant being G10074 and the monoclonal antibody (mAb) using CAP-5D11.

The working concentrations of the encapsulant and mAb were determined by the "checkerboard method". The concentration of the encapsulant (G10074) was diluted at 1:500, 1:1000, 1:2000, 1:4000, 1:8000, 1:16,000, 1:32,000, 1:64,000 times and the CAP-5D11 was diluted in the same concentration gradient. ELISA was performed on CAP, and the antigen and mAb concentrations corresponding to OD_{450 nm} values of 1.5–1.8 were selected as working concentrations. The ELISA method was performed as follows: (1) Encapsulation: The encapsulant (G10074) was diluted to working concentration using Carbonate Buffer, take 100 µL/well of encapsulant solution and added to the enzyme standard plate (incubated for 2 h at 37 °C), and washed 3 times with PBST solution; (2) Closure: 150 µL of BSA solution (5%) was added to each ELISA well and incubated at 37 °C for 1 h; (3) Sample addition: Dilute the CAP standard in PBS, chicken, and egg matrix to 0, 0.11, 0.33, 1, 3, 9, 27 and 81 ng/mL. Add 10 mg of mZIF-8 and shake the adsorption for 20 min, magnetic separation and then re-dissolve using 100 µL of PBS buffer, take 50 µL of the resolution, and add 50 µL of CAP-5D11 to the wells after mixing, incubated at 37 °C for 30 min, and washed three times with PBST solution; (4) Addition of secondary antibody: 100 µL of HRP enzyme-labeled sheep anti-mouse antibody (1:5000 dilution) was added to each well, incubated at 37 °C for 30 min, and washed three times with PBST solution; (5) Color development: 100 µL of the color developer was added to each well, and after 15 min of color development at 37 °C, 50 µL of H₂SO₄ (2.0 M) was added to terminate the color development, and the OD_{450 nm} value was read using an enzyme marker.

After completing the enrichment of CAP in chicken (egg) samples by the no-elution ELISA method using

mZIF-8, the ELISA test is performed after only one wash with pure water. A conventional ELISA (elution procedure required) was used as a control group. The mZIF-8 adsorbed CAP complex was added to 1.0 mL of methanol and vortexed continuously for 20 min. The elution procedure was repeated three times and the eluate was collected. The eluate was blown dry with N₂ and then re-dissolved using PBS aqueous solution for testing. The accuracy and precision of the ELISA method were evaluated using matrix addition recovery and coefficient of variation (RSD), respectively. (See [supplementary material](#) for detailed ELISA methods).

Data analysis — The inhibitory concentration (IC value) of the ELISA is obtained utilizing a four-parameter equation. The concentration of the working solution (standard solution) is the horizontal coordinate and its corresponding absorbance value (OD_{450 nm}) is the vertical coordinate to plot the standard curve. A sigmoidal fit to the test data was performed based on the logistic function in Origin-Lab software (see Eq. 6) to obtain IC₅₀ values and other parameters.

$$Y = \frac{A_1 - A_2}{1 + (x/x_0)^p} + A_2 \quad (6)$$

where Y denotes the measured absorbance value, x denotes the concentration of the substance to be measured; the four parameters are A_1 , A_2 , x_0 , and p , where A_1 denotes the absorbance value measured when the concentration of the substance to be measured is 0; A_2 indicates the absorbance value measured when the concentration of the substance to be measured is infinity; x_0 indicates the concentration of the test substance (IC₅₀) when the absorbance value is 1/2 ($A_1 + A_2$); p is the slope of the S-shaped curve; IC₁₀ value is the detection limit and IC₂₀–IC₈₀ is the detection range.

Actual sample detection

Positive/negative samples were obtained from real samples certified by LC–MS/MS in our laboratory (*National Key Laboratory of Veterinary Public Health Security and Beijing Key Laboratory of Detection Technology for Animal-Derived Food Safety, Beijing, 100193*). Actual sample concentrations of 0, 1, and 3 ng/mL, respectively. Hainan Province sources samples from local supermarkets in Sanya City.

Based on the principle of double-blind testing 24 actual samples (12 samples each of chicken and egg) were pre-treated using mZIF-8 and the residues were determined by an elution-free ELISA method. Comparison of mZIF-8 elution-free ELISA methods using commercial ELISA kits (validation of results using LC–MS/MS).

Supplementary Information

The online version contains supplementary material available at <https://doi.org/10.1186/s44280-023-00016-w>.

Additional file 1: Figure S1. (a) The UV absorption spectrum of CAP; (b) UV quantitative standard curve of CAP. **Figure S2.** (a) Isothermal adsorption curve of ZIF-8; (b) Adsorption kinetic curves of ZIF-8. **Figure S3.** Specificity of mZIF-8 elution-free ELISA for detection of chloramphenicol. **Table S1.** Isothermal adsorption parameters of MOFs. **Table S2.** Adsorption kinetic parameters of MOFs. **Table S3.** Summary of ELISA test results. **Table S4.** Detection results of blind sample addition of real samples. **Table S5.** Test results of chicken and egg samples from supermarkets in Sanya, Hainan Province.

Acknowledgements

This research was supported by the National Key Research and Development Program of China (No. 2020YFF01014605).

Authors' contributions

L.Z. mainly completed the material characterization and ELISA assay part of the work. S.W. completed the design of the specific research proposal and the construction of the material framework, as is the overall writing of the manuscript. J.X. mainly writes and revises manuscripts for the veterinary drug residue section. Y.X. mainly performed the molecular docking simulation and mechanism of action analysis of mZIF-8 and CAP. J.X. used an LC-MS/MS method to validate the assay results. Z. W. completed the preparation of antibodies to chloramphenicol and the identification of antibody immunoreactivity. C.W. optimized the parameters of the immunological method and the evaluation of the assay performance. H.J. guided the idea design of the pre-treatment method and the overall revision of the manuscript. J.S. guided the design idea of the whole study and the completion of the program. The authors read and approved the final manuscript.

Funding

The National Key Research and Development Program of China, 2020YFF01014605, Congming Wu.

Declarations

Ethics approval and consent to participate

Not applicable.

Competing interests

Prof. Jianzhong Shen is Editor-in-Chief and Prof. Zhanhui Wang is Science Editor of *One Health Advances*. They were not involved in the journal's review and decisions related to this manuscript.

Received: 29 April 2023 Revised: 18 May 2023 Accepted: 18 May 2023

Published online: 26 June 2023

References

- Schwarz S, Kehrenberg C, Doublet B, Cloeckaert A. Molecular basis of bacterial resistance to chloramphenicol and florfenicol. *FEMS Microbiol Rev.* 2004;28:519–42. <https://doi.org/10.1016/j.femsre.2004.04.001>.
- Wiest DB, Cochran JB, Tecklenburg FW. Chloramphenicol toxicity revisited: a 12-year-old patient with a brain abscess. *J Pediatr Pharmacol Ther.* 2012;17:182–8. <https://doi.org/10.5863/1551-6776-17.2.182>.
- Kikuchi H, Sakai T, Teshima R, Nemoto S, Akiyama H. Total determination of chloramphenicol residues in foods by liquid chromatography-tandem mass spectrometry. *Food Chem.* 2017;230:589–93. <https://doi.org/10.1016/j.foodchem.2017.03.071>.
- Yibar A, Cetinkaya F, Soyutemiz GE. ELISA screening and liquid chromatography-tandem mass spectrometry confirmation of chloramphenicol residues in chicken muscle, and the validation of a confirmatory method by liquid chromatography-tandem mass spectrometry. *Poult Sci.* 2011;90:2619–26. <https://doi.org/10.3382/ps.2011-01564>.
- Kim J-H, Oh S-W. Pretreatment methods for nucleic acid-based rapid detection of pathogens in food: a review. *Food Control.* 2021;121:107575. <https://doi.org/10.1016/j.foodcont.2020.107575>.
- Plotka-Wasyłka J, Szczepańska N, de la Guardia M, Namieśnik J. Modern trends in solid phase extraction: new sorbent media. *TrAC Trends Anal Chem.* 2016;77:23–43. <https://doi.org/10.1016/j.trac.2015.10.010>.
- Hu B, He M, Chen B. Nanometer-sized materials for solid-phase extraction of trace elements. *Anal Bioanal Chem.* 2015;407:2685–710. <https://doi.org/10.1007/s00216-014-8429-9>.
- Canivet J, Fateeva A, Guo Y, Coasne B, Farrusseng D. Water adsorption in MOFs: fundamentals and applications. *Chem Soc Rev.* 2014;43:5594–617. <https://doi.org/10.1039/C4CS00078A>.
- Dai H, Yuan X, Jiang L, Wang H, Zhang J, Zhang J, et al. Recent advances on ZIF-8 composites for adsorption and photocatalytic wastewater pollutant removal: Fabrication, applications and perspective. *Coord Chem Rev.* 2021;441:213985. <https://doi.org/10.1016/j.ccr.2021.213985>.
- Tanaka S, Fujita K, Miyake Y, Miyamoto M, Hasegawa Y, Makino T, et al. Adsorption and diffusion phenomena in crystal size engineered ZIF-8 MOF. *J Phys Chem C.* 2015;119:28430–9. <https://doi.org/10.1021/acs.jpcc.5b09520>.
- Trino LD, Albano LGS, Granato DC, Santana AG, de Camargo DHS, Correa CC, et al. ZIF-8 metal-organic framework electrochemical biosensor for the detection of protein-protein interaction. *Chem Mater.* 2021;33:1293–1306. <https://doi.org/10.1021/acs.chemmater.0c04201>.
- Zheng G, Chen Z, Sentosun K, Pérez-Juste I, Bals S, Liz-Marzán LM, et al. Shape control in ZIF-8 nanocrystals and metal nanoparticles@ZIF-8 heterostructures. *Nanoscale.* 2017;9:16645–51. <https://doi.org/10.1039/C7NR03739B>.
- Amiripour F, Ghasemi S, Azizi SN. Design of turn-on luminescent sensor based on nanostructured molecularly imprinted polymer-coated zirconium metal-organic framework for selective detection of chloramphenicol residues in milk and honey. *Food Chem.* 2021;347:129034. <https://doi.org/10.1016/j.foodchem.2021.129034>.
- Zhang S, Zhao S, Wang S, Liu J, Dong Y. Development of lateral flow immunochromatographic strips for micropollutant screening using colorants of aptamer-functionalized nanogold particles, part II: experimental verification with aflatoxin B1 and chloramphenicol. *J AOAC Int.* 2018;101:1408–14. <https://doi.org/10.5740/jaoacint.18-0056>.
- Mohamed Idris Z, Hameed BH, Ye L, Hajizadeh S, Mattiasson B, Mohd Din AT. Amino-functionalised silica-grafted molecularly imprinted polymers for chloramphenicol adsorption. *J Environ Chem Eng.* 2020;8:103981. <https://doi.org/10.1016/j.jece.2020.103981>.
- Ma X, Li H, Qiao S, Huang C, Liu Q, Shen X, et al. A simple and rapid sensing strategy based on structure-switching signaling aptamers for the sensitive detection of chloramphenicol. *Food Chem.* 2020;302:125359. <https://doi.org/10.1016/j.foodchem.2019.125359>.
- Zhao X, Zhao H, Dai W, Wei Y, Wang Y, Zhang Y, et al. A metal-organic framework with large 1-D channels and rich OH sites for high-efficiency chloramphenicol removal from water. *J Colloid Interface Sci.* 2018;526:28–34. <https://doi.org/10.1016/j.jcis.2018.04.095>.
- Zhao C, Si Y, Pan B, Taha AY, Pan T, Sun G. Design and fabrication of a highly sensitive and naked-eye distinguishable colorimetric biosensor for chloramphenicol detection by using ELISA on nanofibrous membranes. *Talanta.* 2020;217:121054. <https://doi.org/10.1016/j.talanta.2020.121054>.
- Wang X, Li J, Jian D, Zhang Y, Shan Y, Wang S, et al. Paper-based anti-bi-otic sensor (PAS) relying on colorimetric indirect competitive enzyme-linked immunosorbent assay for quantitative tetracycline and chloramphenicol detection. *Sensors Actuators B Chem.* 2021;329:129173. <https://doi.org/10.1016/j.snb.2020.129173>.
- Jia BJ, He X, Cui PL, Liu JX, Wang JP. Detection of chloramphenicol in meat with a chemiluminescence resonance energy transfer platform based on molecularly imprinted graphene. *Anal Chim Acta.* 2019;1063:136–43. <https://doi.org/10.1016/j.jaca.2019.02.044>.
- Khatamian M, Divband B, Shahi R. Ultrasound assisted co-precipitation synthesis of Fe₃O₄/ bentonite nanocomposite: performance for nitrate, BOD and COD water treatment. *J Water Process Eng.* 2019;31:100870. <https://doi.org/10.1016/j.jwpe.2019.100870>.

22. Li Y, Li P, Ke Y, Yu X, Yu W, Wen K, et al. Monoclonal antibody discovery based on precise selection of single transgenic hybridomas with an on-cell-surface and antigen-specific anchor. *ACS Appl Mater Interfaces*. 2022;14:17128–41. <https://doi.org/10.1021/acsami.2c02299>.
23. Duff DG, Ross SMC, Vaughan DH. Adsorption from solution: an experiment to illustrate the Langmuir adsorption isotherm. *J Chem Educ*. 1988;65:815. <https://doi.org/10.1021/ed065p815>.
24. Umpleby RJ, Baxter SC, Bode M, Berch JK, Shah RN, Shimizu KD. Application of the Freundlich adsorption isotherm in the characterization of molecularly imprinted polymers. *Anal Chim Acta*. 2001;435:35–42. [https://doi.org/10.1016/S0003-2670\(00\)01211-3](https://doi.org/10.1016/S0003-2670(00)01211-3).
25. Simonin JP. On the comparison of pseudo-first order and pseudo-second order rate laws in the modeling of adsorption kinetics. *Chem Eng J*. 2016;300:254–63. <https://doi.org/10.1016/j.cej.2016.04.079>.

Publisher's Note

Springer Nature remains neutral with regard to jurisdictional claims in published maps and institutional affiliations.

Ready to submit your research? Choose BMC and benefit from:

- fast, convenient online submission
- thorough peer review by experienced researchers in your field
- rapid publication on acceptance
- support for research data, including large and complex data types
- gold Open Access which fosters wider collaboration and increased citations
- maximum visibility for your research: over 100M website views per year

At BMC, research is always in progress.

Learn more biomedcentral.com/submissions

